

# Mutations in the *RACGAP1* gene cause autosomal recessive congenital dyserythropoietic anemia type III

Gonzalo Hernández,<sup>1,2\*</sup> Lúdia Romero-Cortadellas,<sup>1\*</sup> Xènia Ferrer-Cortès,<sup>1,2</sup> Veronica Venturi,<sup>1</sup> Mercedes Dessy-Rodriguez,<sup>3,4</sup> Mireia Olivella,<sup>5</sup> Ammar Husami,<sup>6,7</sup> Concepción Pérez de Soto,<sup>8</sup> Rosario M. Morales-Camacho,<sup>9</sup> Ana Villegas,<sup>10</sup> Fernando-Ataulfo González-Fernández,<sup>10</sup> Marta Morado,<sup>11</sup> Theodosia A. Kalfa,<sup>7,12</sup> Oscar Quintana-Bustamante,<sup>3,4</sup> Santiago Pérez-Montero,<sup>2</sup> Cristian Tornador,<sup>2</sup> Jose-Carlos Segovia<sup>3,4</sup> and Mayka Sánchez<sup>1,2</sup>

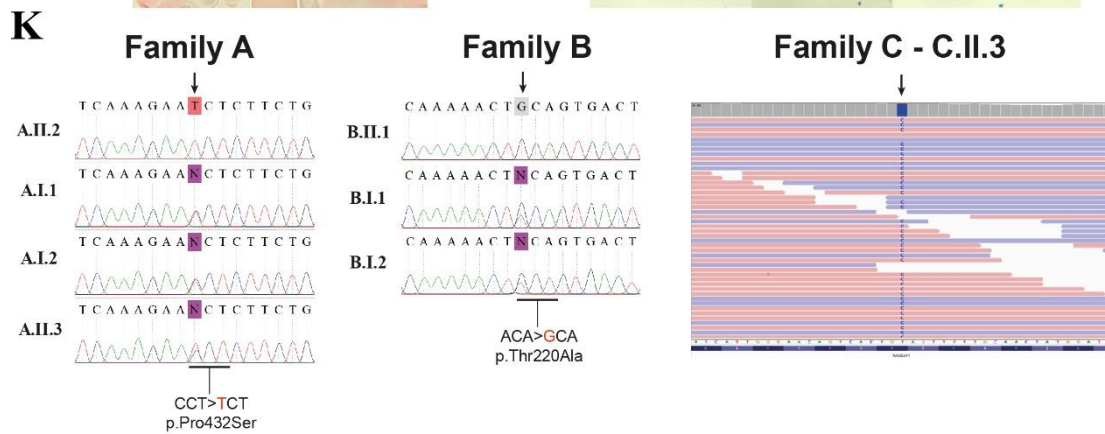
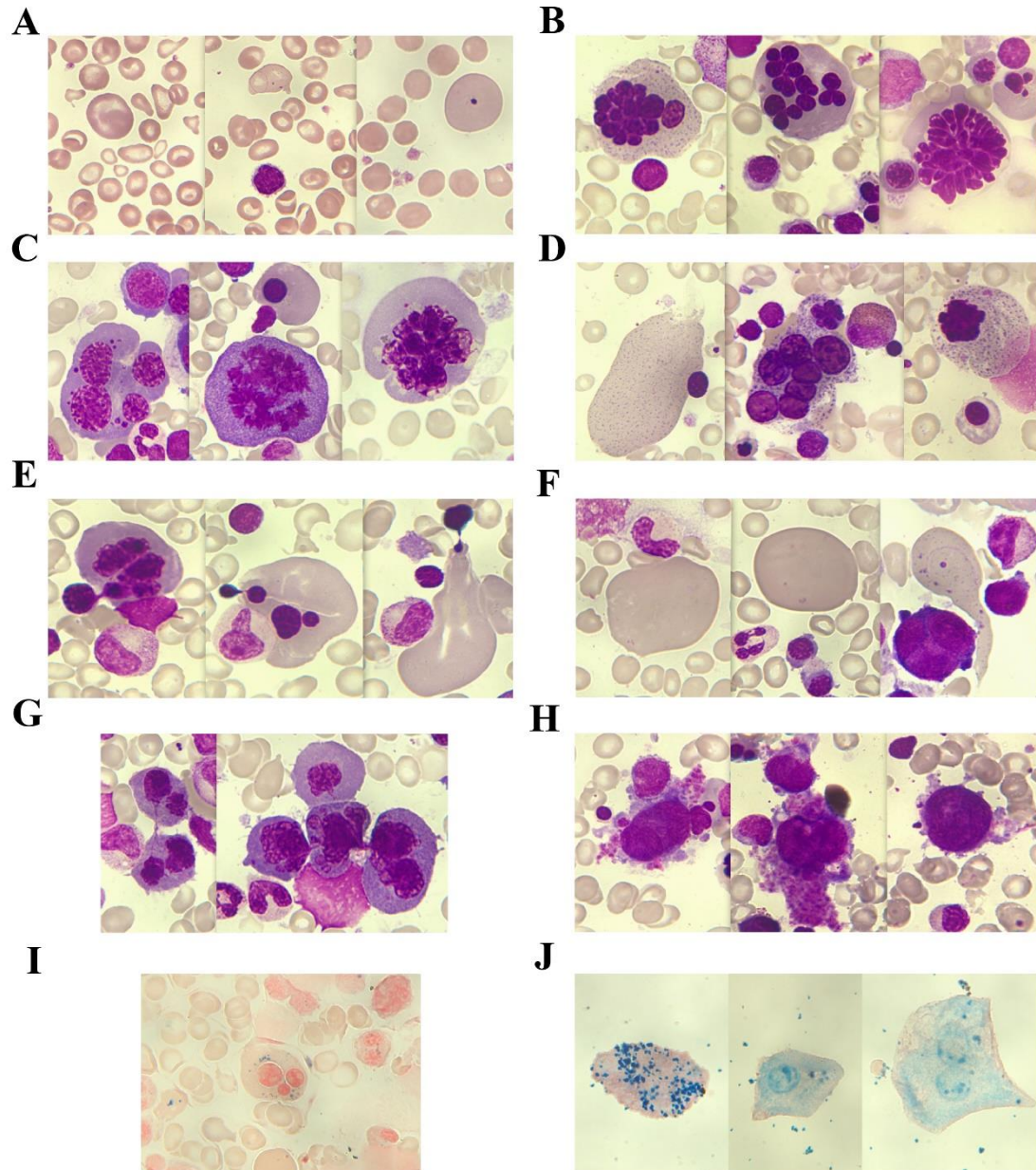
<sup>1</sup>Department of Basic Sciences, Iron metabolism: Regulation and Diseases Group, Universitat Internacional de Catalunya (UIC), Sant Cugat del Vallès, Spain; <sup>2</sup>BloodGenetics S.L. Diagnostics in Inherited Blood Diseases, Esplugues de Llobregat, Spain; <sup>3</sup>Cell Technology Division, Biomedical Innovative Unit, Centro de Investigaciones Energéticas, Medioambientales y Tecnológicas (CIEMAT) and Centro de Investigación Biomédica en Red de Enfermedades Raras (CIBERER), Madrid, Spain; <sup>4</sup>Unidad Mixta de Terapias Avanzadas, Instituto de Investigación Sanitaria Fundación Jiménez, Madrid, Spain; <sup>5</sup>Bioscience Department, Faculty of Science and Technology (FCT), Universitat de Vic – Universitat Central de Catalunya (Uvic-UCC), Vic, Spain; <sup>6</sup>Division of Human Genetics, Cincinnati Children’s Hospital Medical Center, Cincinnati, OH, USA; <sup>7</sup>Department of Pediatrics, University of Cincinnati College of Medicine, Cincinnati, OH, USA; <sup>8</sup>Service of Pediatric Hematology, Hospital Universitario Virgen del Rocío, UGC HH, HHUUVR, Sevilla, Spain; <sup>9</sup>Department of Hematology, Hospital Universitario Virgen del Rocío, Instituto de Biomedicina de Sevilla (IBIS/CISC/CIBERONC), Universidad de Sevilla, Sevilla, Spain; <sup>10</sup>Department of Hematology, Hospital Clínico San Carlos. Universidad Complutense, Madrid, Spain; <sup>11</sup>Department of Hematology, Hospital La Paz, Madrid, Spain and <sup>12</sup>Division of Hematology, Cincinnati Children’s Hospital Medical Center, Cincinnati, OH, USA

*\*GH and LR-C contributed equally as co-first authors.*

Correspondence: M. SÁNCHEZ - msanchezfe@uic.es

<https://doi.org/10.3324/haematol.2022.281277>

**Supplementary Figure S1. peripheral blood, bone marrow, and urine sediment cell images from patient A.II.2 (p.Pro432Ser) and mutation validation of all patients.** BM = Bone Marrow. All pictures were taken with a magnification of 1000X. (A) Peripheral blood (Magnification 1000x). *Left*, anisopoikilocytosis, anisochromia. *Center*, a large erythrocyte with a Cabot ring and Pappenheimer bodies. *Right*, a macroovalocyte with a Howell-Jolly body. (B) Bone marrow (Magnification 1000x). Erythroblasts with >12 nuclei (left and center). On the right, a hyperlobulated element. (C) BM. Erythroblast with four nuclei and chromatin remains (left). Multipolar mitosis (center). Multinucleated erythroid form in karyorrhexis (right). (D) BM. Prominent basophilic stippling in a giant erythrocyte that has just lost its nucleus (left) and in different precursors of erythropoiesis (center and right). (E) BM. Nuclear extrusion images. (F) BM. Giant erythrocytes (left and center). On the right, a large, misshapen red cell shows a Cabot ring, basophilic stippling and probable chromatin remains. (G) BM. Erythroblasts in mitosis with manifestly pathological internuclear bridges, especially in the right image. (H) BM. Small, platelet-forming megakaryocytes. (I) BM. Pathological sideroblasts with Perls Prussian blue staining. (K) Epithelial renal tubule cells from urine sediment stained with iron Perls Prussian blue (MGG 1000x). Cells are iron-loaded indicating hemosiderinuria. (J) Sanger chromatograms of the Families A and B. WES data from Patient C.II.3 covering *RACGAP1* Exon 10. Sixty of sixty-three full-length reads have C instead of T (G replacing A on opposite strand), leading to a missense mutation (ACA→GCA) and substitution of Thr to Ala at amino acid 220. Thirty-three reads for 5' to 3' DNA strand (red) and twenty-seven for reverse-complement DNA strand (blue). Numbering of the subjects is according to the pedigree shown in Figure 1A.



**Supplementary Table S1. Clinical, biochemical and genetic data of patients affected by autosomal recessive CDA III.** F, Female. M, Male. mo, months. n.a., Not Available, PAS, Periodic acid–Schiff stain. (a) Data at birth from patient A.II.2, (b) Data at 3 months of age from patient A.II.2 and 4-5 months of age from patient B.II.1, (c) Data at 18 months of age from patient A.II.2, (d) Data at 10 years of age from patient A.II.2, (e) Most recent data at 17-18 years of age from patient A.II.2 and 35 years of age from patient B.II.1. (f) Data at 5 years of age from patient B.II.1. (g) Transfusion threshold during childhood for patient C; after 24 years of age, he was started on chronic transfusion regimen every 4 weeks in order to maintain Hb trough > 100 g/L. (h) At 32 years of age. He had chelation with deferoxamine subcutaneous nightly infusion 5 nights/week at 12-18 years of age, deferoxamine continuous IV infusion via central line at 25 years of age for 9 months, and then deferasirox 1500 mg daily starting at 26 years of age up to 34 years of age when he received hematopoietic stem cell transplant. (i) Reported by the patient since childhood. (j) Azoospermia reported at 24 years of age by the patient. (k) Data from January 2022 from patient B.II.1.

<i>Parameter and units</i>	<i>Family A - Patient II.2</i>	<i>Family B - Patient II.1</i>	<i>Family C- Patient II.3</i>	<i>Normal values</i>
<b>Sex</b>	M	F	M	
<b>Age at clinical diagnosis</b>	At birth	4 mo.	4 m.o.	
<b>Current age (years)</b>	18	35	40	
<b>Hemoglobin, Hb (g/L)</b>	67 (a)	74 (b)	60 (g)	105-145
	106 (e)	96-101 (e)		120-156 (Adult)
<b>MCV (fl)</b>	126 (a)	74 (b)	n.a.	70-108
	107 (e)	123 (e)		80-99 (Adult)
<b>Red blood cells (/L)</b>	1,6 x 10 <sup>12</sup> (a)	1.09 x 10 <sup>12</sup> (b)	n.a.	3.3-4.5
	3.1 x 10 <sup>12</sup> (e)	2.39 x 10 <sup>12</sup> (e)		3.90- 5.20 (Adult)
<b>Reticulocytes (%)</b>	1.87 (e)	2.14 (e)	n.a.	

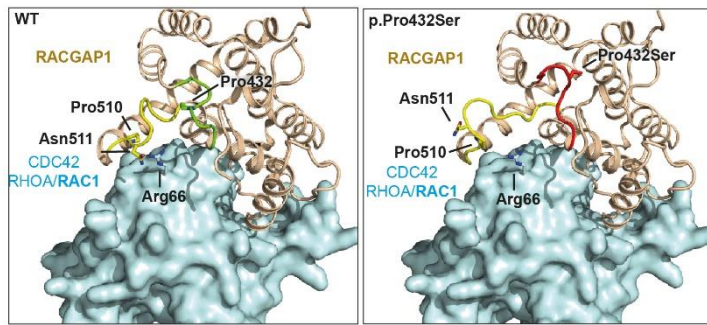
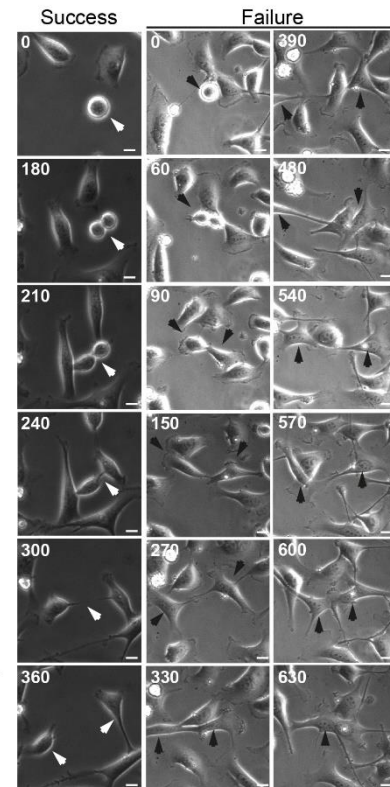
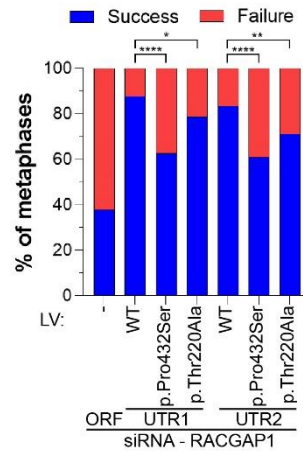
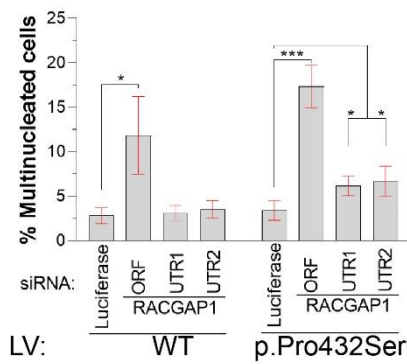
<b>Total bilirubin</b>	14.2 (a)	2.7 (b)	n.a.	0.30-
<b>(mg/dL)</b>	3.9 (e)	1.15 (e)		1.20
<b>Indirect bilirubin</b>	4.18 (a)	2 (b)	n.a.	<0.3
<b>(mg/dL)</b>	3.4 (e)	0.58 (e)		
<b>LDH (UI/L)</b>	1410 (c)	554 (b)	n.a.	150-350
	1443 (e)	987 (k)		
<b>Haptoglobin (mg/dL)</b>	<0.1 (c)	<1 (k)	n.a.	40-280
	<0.1 (e)			
<b>Serum iron (mg/dL)</b>	166 (b)	164 (e)	n.a.	50-170
	98 (c)			
	173 (e)			
<b>Serum ferritin</b>	547 (b)	97 (e)	730 (h)	10-291
<b>(µg/dL)</b>	94 (c)			
	174 (e)			
<b>Erythropoietin</b>	117 (c)	n.a.	n.a.	4-30
<b>(mU/L)</b>				
<b>Transferrin</b>	96 (b)	52	n.a.	20-45
<b>saturation (%)</b>				
<b>Hepcidin ng/ml</b>	1.06 (e)	1.50 (e)	n.a.	
<b>Coombs test</b>	Negative (b)	n.a.	Negative	
<b>Virus</b>	Negative: parvovirus B19, CMV- IgM, HBV (hepatitis B) (b)	n.a.	n.a.	
<b>Hemosiderinuria</b>	Yes (d)	n.a.	n.a.	
<b>Fetal Hemoglobin</b>	2.9 (d)	15 (b)	n.a.	
<b>(%)</b>	2.9 (e)	3 (f)		
<b>Peripheral blood</b>	Severe anisopoikilocytosis, macrocytic forms, anisochromia, basophilic stippling, Howell-Jolly bodies, Cabot's ring and Pappenheimer bodies, erythroblasts (1/100 leukocytes) (b)	Marked morphological disorders in the red cell series with macrocytosis, red cell fragmentation and basophilic stippling and isolated inclusion bodies with brilliant cresyl blue (b)	n.a.	
<b>Bone marrow. Light microscope</b>	Erythroid hyperplasia, multinucleated erythroblasts, gigantoblasts and megaloblastic changes, karyorrhexis, internuclear bridges, increased hemosiderin	Hyperplasia of the red cell series (M/E ratio=1:4). Giant normoblasts with >10 nuclei, megaloblastosis, karyorrhexis, abnormal hemoglobinization,	Erythroid hyperplasia and dyserythropoiesis with large multinucleated erythroblasts (35% of the erythroid	

	iron in macrophages (3-4*), pathological sideroblasts (28 %), ring sideroblasts (8 %).	increased iron storage with 70% sideroblasts (no ring) (b)	precursors with three to six nuclei per cell.
<b>Bone marrow.</b>	n.a.	Erythroblasts with irregular nuclei. Abnormally electron-dense heterochromatin, blebs and clefts within the nuclear region. Folds of membrane with double perinuclear spaces, absence of the nuclear membrane in certain points. Intracytoplasmic myelin figures and large intracytoplasmic myelin masses of electron-dense granular material of precipitated globin chains.(b)	n.a.
<b>Electron microscope</b>			
<b>Others</b>	Skull hair-on-end appearance (c) Splenohepatomegaly at birth (a). Splenohepatomegaly of 3 cm at present age (e) No gallstones (d) No ophthalmological defects (d)	Skull defects secondary to increased medullary erythropoiesis <sup>5</sup> . Splenohepatomegaly. Splenectomy at age 9 y.o. Cholecystectomy secondary to biliary lithiasis age 25 y.o. No ophthalmological defects (e) Antiphospholipid syndrome, papillary thyroid cancer.	Visible skull bone hyperplasia secondary to increased erythropoiesis. Splenohepatomegaly. Splenectomy at 12 y.o. due to splenohepatomegaly. Poor vision (i) Stunted growth (adult height 162 cm) Infertility (j)
<b>Red blood cells transfusions</b>	Only 3 transfusions needed at 1 mo. age	Periodic transfusions until splenectomy, after splenectomy sporadic needs	3-4 transfusions/year up to 24 yo.; started monthly transfusions afterwards to maintain Hb trough>100 g/L to suppress ineffective erythropoiesis
<b>Genetics</b>	c.1294C>T; c.1294C>T	c.658A>G; c.658A>G	c.658A>G; c.658A>G
<b>RACGAP1</b> (NM_013277.4 ; NP_037409.2)	p.Pro432Ser; p.Pro423Ser	p.Thr220Ala; p.Thr220Ala	p.Thr220Ala; p.Thr220Ala

**Supplementary Figure S2. Functional and modelling studies of RACGAP1 mutations.** (A)

Wild-type RACGAP1-CDC42/RAC1/RHOA complex conformation model (*left*). Pro432 is located in the 429-437 residue loop (green) that interacts with a second loop, residues 505-513 (yellow). In the 505-513 RACGAP1 loop (yellow), Pro510 and Asn511 interact with Arg66 from CDC42 and RAC1 and with Arg68 in the case of RHOA. *Right*, mutated p.Pro432Ser RACGAP1-CDC42/RAC1/RHOA complex conformation model. The introduction of the Pro432Ser mutation modifies the conformation of the 429-437 residue loop (red) and substantially alters the conformation of the 505-513 loop (yellow), causing it to lose the interaction with the Arg66/68 residue from CDC42, RAC1 and RHOA. Overall, the local structural change induced by p.Pro432Ser mutation may destabilize complex formation of RACGAP1 with GTPases CDC42/RAC1/RHOA. The RACGAP1 model is depicted as ribbons in gold, except for loop 505-513 that is depicted in yellow and loop 429-437 that is shown in green in the wt conformation (*left*) and in red in the mutated conformation (*right*). CDC42, RAC1 and RHOA are shown as surface in cyan. Model was based on the RACGAP1 (GAP domain)-RAC1 complex. (B) Bright field images of HeLa cells treated with siRNA targeting *RACGAP1* (siRACGAP1-ORF). Upper panel shows a cell that undergoes normal cytokinesis (recorded as “success”), while lower panels show a cell that after division undergoes furrow regression leading to a binucleated cell (recorded as “failure”). Indicated times are in minutes. Dividing cells are indicated by black or white arrows. Scale bars represent 10  $\mu$ m. (C) Time-lapse data quantification from (B) in HeLa cells stably expressing WT, p.Pro432Ser or p.Thr220Ala RACGAP1-myc (endogenous levels of RACGAP1 protein were eliminated by 2 independent siRNAs targeting the 3'-UTR of *RACGAP1*, i.e., siRACGAP1-UTR1 and siRACGAP1-UTR2) shows that both mutations cause an increase in cytokinesis failure compared with cells with the WT form (n=76-96 from two different pooled experiments). CI was calculated (Wilson-Brown method) to compare distributions of the number of metaphases succeeding in completing or failing to complete cytokinesis. (D) Quantification of at least three different cytometry experiments in which a significant increase in multinucleation was observed in HeLa cells expressing the p.Pro432Ser mutation determined by the DNA content of the cells. Bars represent the mean  $\pm$  SD. Student's

T-test was performed to compare multinucleation levels in cells treated with each siRNA in comparison with cells treated with a control Luciferase siRNA. (E) Cytospin images of cells undergoing erythroid differentiation at day 9 and 14 from the controls, A.II.2 patient and A.II.2 patient transduced with 40  $\mu$ L of virus. Cell size decreases between days 9 and 14. Black arrows denote cells with more than 2 nuclei and white arrows show macrocytic erythrocytes in the A.II.2 patient.

**A****B****C****D****E**